Proc. Natl. Acad. Sci. USA
Vol. 81, pp. 3723–3727, June 1984
Biophysics

Application of the Dale–Eisinger analysis to proximity mapping in the contractile system

(anisotropy decay/muscle proteins/energy transfer)

PETER M. TORGERSON AND MANUEL F. MORALES

Cardiovascular Research Institute, University of California, San Francisco, CA 94143

Contributed by Manuel F. Morales, March 5, 1984

ABSTRACT **Fluorescence anisotropy decays were used to quantify the degree of rapid librational motion associated with several fluorescent probes attached to contractile proteins. This information allows an analysis of how far κ^2, the resonance energy transfer orientation factor, may deviate from the dynamically averaged value of 2/3. Extrema can then be set on R_0, the critical transfer distance, and hence on the interprobe distance. These results set maximum ranges on possible distances between several probe pairs used in the mapping of contractile protein structure by resonance energy transfer.**

Resonance energy transfer measurements of interpoint distances have recently played an important role in deducing the spatial arrangement of the multiprotein complexes in contractile systems. The method is capable of providing information on the separation between two well-defined sites. This is particularly useful in muscle research, given the large number of chemically distinguishable locations on myosin, actin, and associated proteins and the current lack of x-ray crystallographic information. Enough information is available now so that a lattice of several defined points can be constructed and this lattice related to other structural information available on muscle proteins (1). Of the experimental factors necessary for an energy transfer distance estimate, the hardest to get is κ^2, the "orientation" factor. In general, the actual value of κ^2 is not experimentally measurable. The simplest approximation is to assume that both donor and acceptor transition dipoles are undergoing motion that randomizes the orientations much faster than the donor is decaying to its ground state. The randomization must be due to each probe sampling all orientations, not due to a static random distribution of probes. In the first case, the dynamically averaged isotropic limit holds, and $\kappa^2 = 2/3$. In general, the possible range of dipole motion is restricted when a fluorophore is bound to a protein; then this approximation becomes questionable. It can still be used, but then it is desirable to know how much uncertainty this contributes to the distance estimate. Several discussions of this problem have appeared in recent years (2–4). In the sense of quantification the most useful analysis is that of Dale *et al.* (5). These authors use the decrease in the zero-time value in a fluorescence anisotropy decay curve to estimate the degree of rapid probe randomization. This information then allows calculation of upper and lower bounds on κ^2, and hence on R_0, the critical transfer distance, and on R, the interprobe distance. Some recent applications of the method have appeared (6, 7). Here we apply the analysis to examine the uncertainties in several recent distance measurements made on the contractile system and relate these uncertainties to the reliability of protein structure mapping by resonance energy transfer (1).

The publication costs of this article were defrayed in part by page charge payment. This article must therefore be hereby marked "*advertisement*" in accordance with 18 U.S.C. §1734 solely to indicate this fact.

MATERIALS AND METHODS

Proteins. Myosin was prepared from rabbit back muscle according to Tonomura *et al.* (8). Myosin subfragment 1 (S1) was prepared by using chymotrypsin (9) and was purified by either filtration through Sephacryl S-200 in 50 mM tris(hydroxymethyl)aminomethane/0.1 mM sodium azide, pH 7.5, or ion-exchange chromatography on DE-52 in 75 mM imidazole at pH 7.0 eluted with a KCl step gradient at 5, 50, and 120 mM. The quality of the preparation was monitored by $NaDodSO_4$/polyacrylamide gel electrophoresis and by measuring the Ca^{2+} and K^+/EDTA ATP activities. Actin was purified from rabbit back and white hind leg muscle acetone powder (10).

N-(iodoacetyl)-*N'*-(5-sulfo-1-naphthyl)ethylenediamine (1,5-IAEDANS) (11), 5-(iodoacetamido)fluorescein (IAF), and iodoacetyl-salicylic acid (IAS) were products of Molecular Probes (Plano, TX); 2,4,6-trinitrobenzenesulfonate was a product of Aldrich Chem (Metuchen, NJ). *N*-(iodoacetyl)-*N'*-(8-sulfo-1-naphthyl)ethylenediamine (1,8-IAEDANS) was obtained from Sigma. S1 labeled at its reactive thiol ("SH_1") with IAF at the reactive sulfhydryl SH_1 (IAF-S1) and actin labeled at cysteine-374 with IAEDANS (IAEDANS-actin) were prepared essentially according to Takashi (12). Initial purification of IAF-S1 was by filtration on Sephadex G-50, followed by overnight dialysis to remove nonspecifically bound fluorescein. Protein concentrations were estimated from optical density measurements on unlabeled samples, using $A^{1\%}_{280} = 7.5$ for S1 (13) and $A^{1\%}_{290} = 6.3$ for actin (14). Concentrations of labeled proteins were assayed by the Folin-phenol method using the unlabeled protein as a standard. Labeling of the reactive lysine residue of S1 with trinitrobenzenesulfonate was according to Takashi *et al.* (15) and labeling of the light chain 3 thiol followed by the exchange of labeled for unlabeled light chains on S1 was as in Marsh and Lowey (16).

Fluorescence Measurements. Two instruments were used to make time-resolved fluorescence anisotropy measurements. Early experiments were done on the "double-beam" fluorescence polarization decay apparatus described by Mendelson *et al.* (17). Later experiments were done on an instrument that incorporated the same data acquisition electronics, with pile-up rejection hardware removed, but with a shorter lamp flash and with a sample cavity, optical train, and cooled phototube supplied by Photochemical Research Associates (London, ON, CAN). Excitation and emission

Abbreviations: S1, myosin subfragment 1; 1,5-IAEDANS, *N*-(iodoacetyl)-N'-(5-sulfo-1-naphthyl)ethylenediamine; 1,8-IAEDANS, *N*-(iodoacetyl)-*N'*-(8-sulfo-1-naphthyl)ethylenediamine; IAF, 5-(iodoacetamido)fluorescein; SH_1, fast-reacting thiol on the heavy chain of myosin; IAS, iodoacetylsalicylic acid; 1,5- or 1,8-IAEDANS-LC_3, 1,5- or 1,8-IAEDANS on the sole thiol of myosin light chain 3; TNP-S1, S1 reacted with 2,4,6-trinitrobenzenesulfonate at the "reactive lysine residue"; IAF-S1, IAF on the reactive sulfhydryl SH_1 of S1; IAS-LC_3, IAS on the sole thiol of light chain 3; 1,5-IAEDANS-actin, 1,5-IAEDANS on cysteine-373 of actin.

wavelengths were selected by interference and cut-off filters. Data collection was under the control of a DEC PDP8/e computer. Since this is an L-format instrument—that is, it has a single phototube at right angles to the excitation beam—anisotropy data were collected by accumulating several successive data sets for short periods, alternating the emission polarizer between vertical and horizontal orientations, and later summing the polarized intensities in the computer. This procedure serves to reduce the effect of slow instrumental drifts in either intensity or time. Variations in the photomultiplier tube time response with wavelength were estimated by reanalyzing the data after shifting the lamp in time relative to the data and monitoring the change in the goodness of fit. Data in the PDP8/e were transferred to a Data General Eclipse 230S computer for further analysis.

The emission anisotropy is

$$r(t) = [I_{VV}(t)G - I_{HV}(t)]/[I_{VV}(t)G + 2I_{HV}(t)] \quad [1]$$
$$= s(t)/d(t),$$

where $s(t)$ and $d(t)$ are the sum (total intensity) and difference curves, respectively, H and V are horizontal and vertical polarizer orientations, respectively, and $G = I_{HH}/I_{VH}$ is the correction factor for the difference in phototube response as a function of emission polarizer orientation. The first subscript refers to the emission polarizer orientation and the second to the excitation polarizer. G was measured by rotating the excitation polarizer to the horizontal and measuring the steady-state intensities of the sample (18) or of a quinine sulfate solution with an expected anisotropy of nearly zero.

The analysis procedure is that described by Rose *et al.* (18). The sum, anisotropy, and difference responses upon excitation by an infinitely narrow lamp flash are, respectively,

$$s(t) = \Sigma_i \alpha_i \exp(-t/\tau_i) \quad [2]$$
$$r(t) = \Sigma_j \beta_j \exp(-t/\phi_j) \quad [3]$$
$$d(t) = s(t) \cdot r(t), \quad [4]$$

where τ_i are the fluorescence lifetimes, ϕ_j are the rotational correlation times, and α_i and β_j are their associated pre-exponential terms. The lifetime response parameters are first obtained by analyzing $s(t)$. These parameters are then held constant in Eq. 4 and the anisotropy parameters are extracted. The zero-time anisotropy is then $r(0) = \Sigma\beta_j$. Deconvolution from the finite-width lamp pulse and multiexponential analysis were carried out by the nonlinear least-squares iterative reconvolution technique (19, 20), using programs based on routines given to us by L. Brand.* Goodness of fit was judged by the reduced χ^2, the percent residuals, and the autocorrelation of the weighted residuals.

The observed zero-time anisotropies were further corrected for inaccuracies due to the imperfect polarization of light by the film polarizers, based on an analysis (20) of the polar-

*The present version of these analysis routines is implemented in Data General Fortran V, employing an Eclipse 230S computer and Tectronix Plot 10 graphics software, and is available on request.

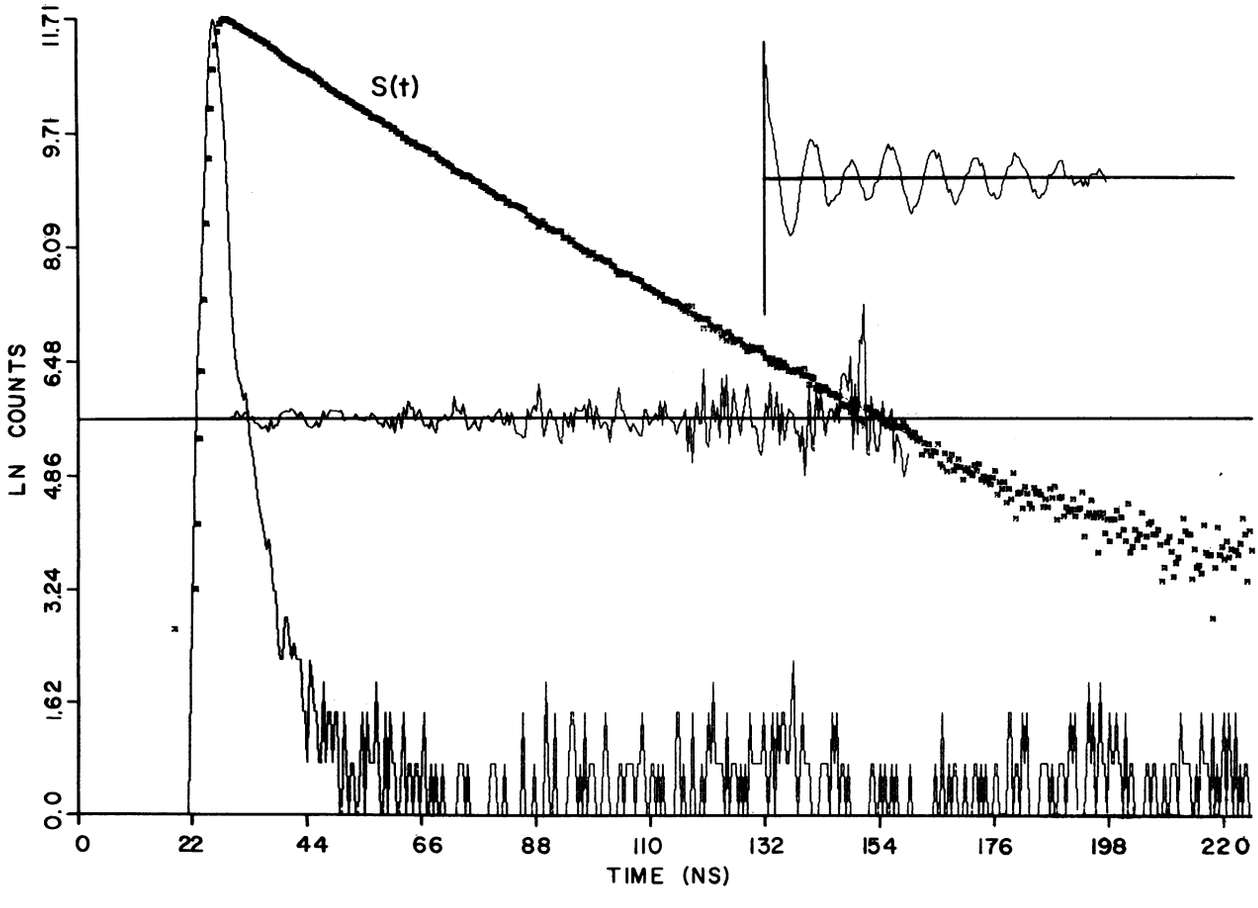

FIG. 1. Total intensity of 6 nM 1,5-IAEDANS-actin and 3 nM S1 at 4°C. The lamp and sum curves are shown in semilogarithmic form. The percent residuals are shown in a linear scale over the data analysis range. The autocorrelation of the weighted residuals, plotted over one-half the data analysis range, is shown in the *Inset*. The best fit is $\alpha_1 = 0.38$, $\tau_1 = 14.6$ ns, $\alpha_2 = 0.62$, $\tau_2 = 23.1$ ns, with $\chi^2 = 2.09$. For this data set, the lamp contained nitrogen at one-half atmosphere. Excitation was through a 380-nm interference filter with a 10-nm bandwidth, and emission was viewed from 430 to 570 nm, selected with a pair of high- and low-pass filters. No lamp time-shift correction was necessary.

ization scrambling caused by the birefringence of quartz windows. For an L-format instrument (21),

$$r' = r(1 - 3a), \quad [5]$$

where r is the true anisotropy, r' is the observed anisotropy, and a is the scrambling coefficient, obtained by measuring r' on a sample with a known r. The correction in practice was small ($a < 0.02$) at the wavelengths employed here. Anisotropies in the absence of probe motion were obtained from samples in 90% glycerol at −50°C.

Theory. In the model underlying the Dale *et al.* (5) analysis, donor and acceptor dipoles whirl in respective cones having fixed symmetry axes between which transfer occurs. In general, an experimentally observed zero-time anisotropy is the anisotropy corresponding to a static random distribution (2/5 when absorption and emission dipoles are collinear), multiplied by a "depolarization factor." If the depolarization results from successive processes, the "factor" is the continued product of factors, each corresponding to a component process. Thus, in the model the overall depolarization—i.e., that of the donor emission when acceptor is excited—results from three successive processes: donor motion, transfer from donor axis to acceptor axis, and acceptor motion. The analysis then uses these values to set upper and lower bounds on the possible values of κ^2. Following the Dale *et al.* notation, the axial depolarization factors, $\langle d_\xi^x \rangle^2$—where ξ stands for either donor, D, or acceptor, A—are given by

$$r_\xi(0)/r_f = \langle d_\xi^x \rangle^2, \quad [6]$$

where r_f is the anisotropy of a rigid ensemble of probes. The axial transfer depolarization factor, d_T^x, can be obtained from the above two depolarization factors and from the time dependence of the anisotropy of the transferred intensity. Dale *et al.* also derive that if both axial depolarization factors are positive (which is certain when they are >0.5) and if the transfer depolarization is unknown, then the limiting values of κ^2 can be calculated directly rather than from their contour plots:

$$\langle \kappa^2 \rangle_{max} = (2/3)(1 + \langle d_D^x \rangle + \langle d_A^x \rangle + 3\langle d_D^x \rangle \langle d_A^x \rangle)$$
$$\langle \kappa^2 \rangle_{min} = (2/3)[1 - (\langle d_D^x \rangle + \langle d_A^x \rangle)/2]. \quad [7]$$

These cases correspond to the most favorable (both dipoles parallel to each other and to the vector connecting them) and least favorable (both dipoles perpendicular to their connecting vector and to each other) orientations of the average donor and acceptor dipoles, respectively. The limits to R_0 are then given by

$$R_{0,\,min,\,max} = [3/2(\langle \kappa^2 \rangle_{min,\,max})]^{1/6} R(2/3). \quad [8]$$

The average cone angle θ sampled by the probe during azimuthal orientational averaging is given by

$$\langle d_\xi^x \rangle = (3/2)\langle \cos \theta \rangle^2 - 1/2. \quad [9]$$

RESULTS AND DISCUSSION

Six different labelings were used in this study: 1,5-IAEDANS on cysteine-373 of actin (1,5-IAEDANS-actin), IAF

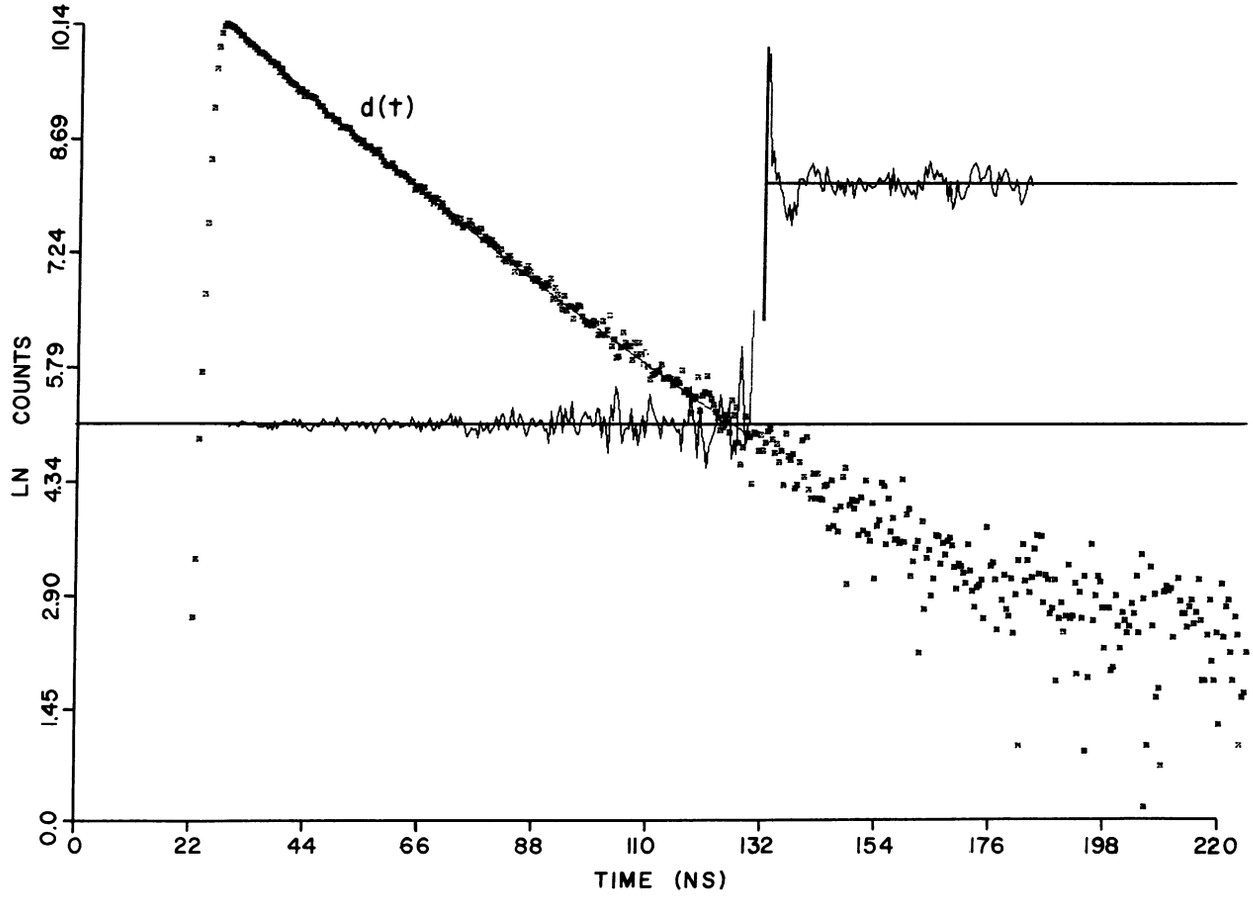

FIG. 2. Difference analysis of the data of Fig. 1, in a semilogarithmic plot. Percent residuals and autocorrelation are shown as before. The best fit is $\beta_1 = 0.048$, $\phi_1 = 11.4$ ns, $\beta_2 = 0.256$, $\phi_2 = 266$ ns, with $\chi^2 = 1.16$.

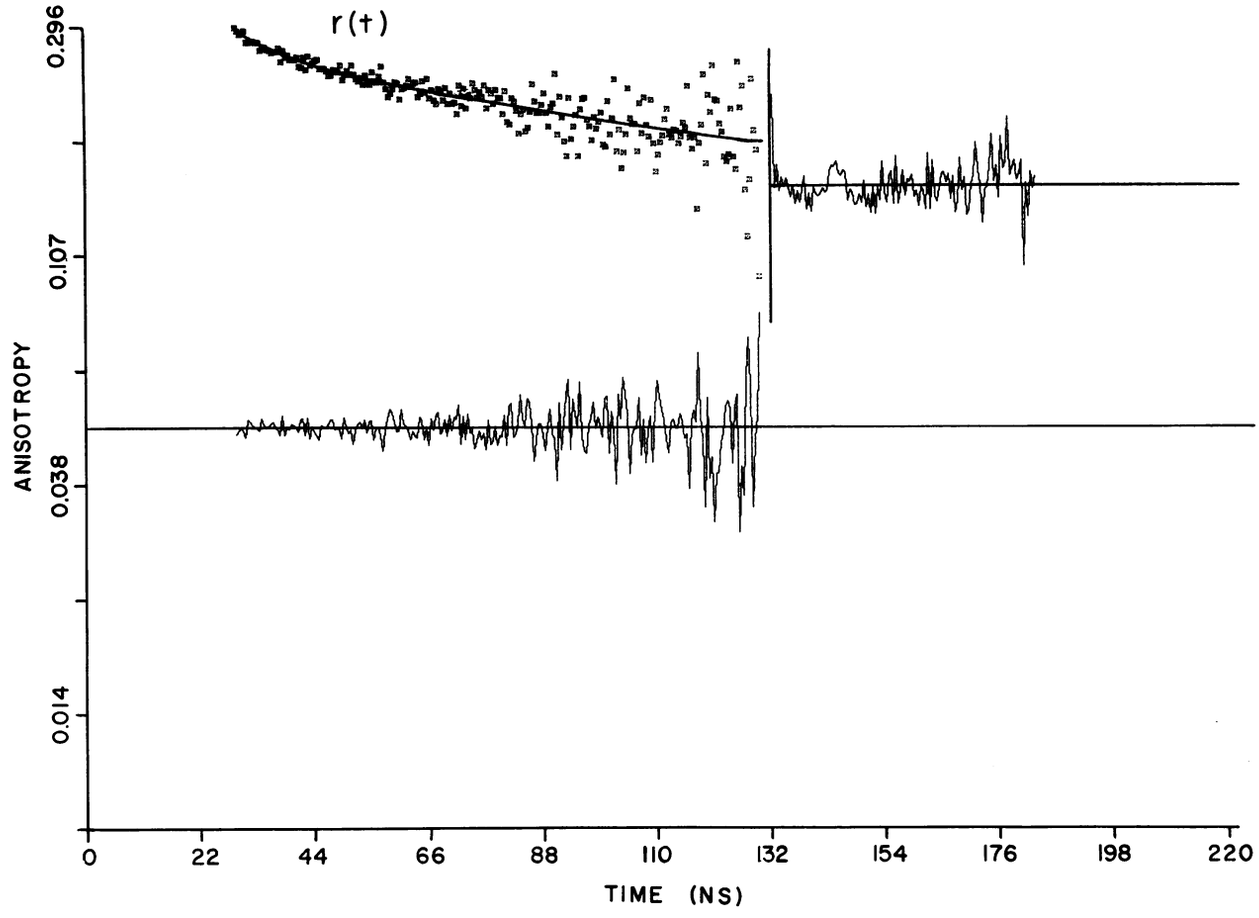

FIG. 3. Logarithmic representation of the anisotropy decay, synthesized from the sum and difference parameters derived in Figs. 1 and 2.

on the reactive sulfhydryl "SH_1" (fast-reacting thiol on the heavy chain of myosin) of S1 (IAF-S1), IAS on the sole thiol of light chain 3 (IAS-LC_3), 1,5- or 1,8-IAEDANS on the same thiol (1,5- or 1,8-IAEDANS-LC_3), and trinitrobenzenesulfonate on the reactive lysine residue of S1 (TNP-S1). These labelings allow analysis of five recently determined interprobe distances in these proteins. A representative data set for 1,5-IAEDANS-actin is given in Figs. 1–3. Shown are the lamp, total intensity, difference, and anisotropy curves, along with their associated percent residuals and residual autocorrelation curves. A synopsis of the five fluorescent labelings is in Table 1. The local motions vary from the largely immobilized case of 1,5-IAEDANS-actin to the highly mobile case of 1,5- or 1,8-IAEDANS-LC_3. The sum of the β_js of the decay of 1,5-IAEDANS-actin in the presence of S1 are in good agreement with those observed by Ikkai *et al.* (22) for a similar set of conditions. Table 2 gives the extrema of κ^2 and of R_0 relative to $R_0(2/3)$, calculated according to Eqs. **7** and **8**. Unfortunately, the transfer depolarization factors for these cases could not be measured. In the 1,5-IAEDANS-actin:IAF-S1 case, the large background due to the tail of the 1,5-IAEDANS-actin emission and to direct excitation of the fluorescein (together accounting for about 90% of the intensity) precludes collection of reliable transfer anisotropy data. In the cases in which trinitrobenzenesulfonate is the acceptor there is no emission, thus preventing the determination of both $\langle d_A^x \rangle$ and $\langle d_T^x \rangle$.

The first case in Table 2 (1,5-IAEDANS-actin and IAF-S1) shows that even restricted probe motion can reduce the κ^2 uncertainty. This case was studied by Takashi (12); the $R(2/3)$ is 6.0 nm. The lower and upper bounds are therefore 4.2 nm and 7.9 nm. This range may seem large, but it should be remembered that 4.2 and 7.9 are absolute bounds, not half-widths of distributions, and consequently it is certain that the two probes are at least 4.2 nm apart. The present analysis considers only the effect of probe motion in promoting $\kappa^2 \rightarrow 2/3$. Other effects, such as multiplicity in the acceptor absorption transition dipole, would reduce the κ^2 uncertainty further. Variations in the excitation polarization spectrum of the donor (19) have no effect on κ^2, since rapid vibronic relaxation to the same lowest-level excited singlet state occurs regardless of excitation pathway, and hence there is a well-defined emission dipole orientation. In cases in which IAEDANS is the acceptor, however, the multiplicity of absorption dipole orientations could significantly reduce the range of κ^2, depending on the exact region of spectral overlap.

The second through fourth examples illustrate that the κ^2

Table 1. Anisotropy decay parameters

Sample	β_1	ϕ_1	β_2	ϕ_2	χ^2	$r(0)$	r_f	$\langle d^x \rangle$	θ
1,5-IAEDANS-actin	0.052	15	0.260	198	1.11	0.340	0.376	0.951	10.4
IAF-S1	0.079	13.0	0.190	∞	0.76	0.292	0.40	0.854	18.2
IAS-LC_3	0.072	25.4	0.132	144	1.154	0.205	0.383	0.732	25.0
1,5-IAEDANS-LC_3	0.176	2.6	0.144	80.7	1.792	0.153	0.376	0.638	29.4
1,8-IAEDANS-LC_3	0.105	1.03	0.149	130.8	1.13	0.161	0.369	0.661	28.4

Table 2. Upper and lower bounds for energy transfer parameters

Donor	Acceptor	κ^2_{min}	κ^2_{max}	R_0(min)	R_0(max)
1,5-IAEDANS-actin	IAF-S1	0.065	3.49	0.678	1.318
1,5-IAEDANS-LC_3	TNP-S1	0.121	3.03	0.752	1.287
IAS-LC_3	TNP-S1	0.089	3.29	0.715	1.305
1,8-IAEDANS-LC_3	TNP-S1	0.113	3.10	0.744	1.292
1,5-IAEDANS-LC_3	IAF-S1	0.169	2.75	0.796	1.266

R_0(min) and R_0(max) are expressed relative to $R_0(2/3)$.

indeterminacy can be greatly reduced when significant motion of one probe exists even though the motion of the other is unmeasurable. In these cases, the upper and lower bounds define a conservative maximum range since almost certainly at least some rapid motion occurs in the acceptor.

The final case is similar to that reported by Marsh and Lowey (16), who measured the energy transfer between SH_1 and the sulfhydryl of light chain 1. Here both probes suffer a large amount of randomization. The absolute minimum of R_0 is only 20% below that of the dynamically averaged limit, and the maximum is only 26% above, so $R(2/3)$ is a good approximation to the true interpoint distance.

In summary, these results illustrate that the local motional freedom of probes used in energy transfer experiments in muscle proteins is found to vary from the immobile to nearly total, thus setting corresponding uncertainty ranges in the distance calculated by using the dynamic isotopic assumption. Although such uncertainty ranges somewhat limit the resolution of the mapping of contractile protein structure by resonance energy transfer as outlined by Botts *et al.* (1), they also aid in construction of the map by delineating a possible range of values.

We thank Dr. R. Takashi for providing the labeled light chain samples and Prof. L. Brand for sharing his deconvolution software. We appreciate a critical reading of the manuscript by Prof. L. Brand and Dr. J. Eisinger. This research was carried out during the tenure of a Postdoctoral Fellowship to P.M.T. from the Muscular Dystrophy Association; M.F.M. is a Career Investigator of the American Heart Association. This research was supported by Grants HL-16683, PCM-79-22174, and CI-8.

1. Botts, J., Takashi, R., Torgerson, P., Hozumi, T., Muhlrad, A., Mornet, D. & Morales, M. F. (1984) *Proc. Natl. Acad. Sci. USA* **81**, 2060–2064.
2. Stryer, L. (1978) *Annu. Rev. Biochem.* **47**, 819–846.
3. Fairclough, R. H. & Cantor, C. R. (1978) *Methods Enzymol.* **28**, 347–379.
4. Haas, E., Katchalski-Katzir, E. & Steinberg, I. (1978) *Biochemistry* **17**, 5064–5070.
5. Dale, R. E., Eisinger, J. & Blumberg, W. E. (1979) *Biophys. J.* **26**, 161–194.
6. Cardon, J. W. & Hammes, G. G. (1982) *Biochemistry* **21**, 2863–2870.
7. Cheung, H. C., Wang, C.-K. & Garland, F. (1982) *Biochemistry* **21**, 5135–5142.
8. Tonomura, Y., Appel, P. & Morales, M. F. (1966) *Biochemistry* **5**, 515–522.
9. Weeds, A. G. & Taylor, R. S. (1975) *Nature (London)* **257**, 54–56.
10. Spudich, J. & Watt, S. (1971) *J. Biol. Chem.* **246**, 4866–4871.
11. Hudson, E. N. & Weber, G. (1973) *Biochemistry* **12**, 4154–4161.
12. Takashi, R. (1979) *Biochemistry* **18**, 5164–5169.
13. Wagner, P. D. & Weeds, A. G. (1977) *J. Mol. Biol.* **109**, 455–470.
14. Houk, W. & Ue, K. (1974) *Anal. Biochem.* **62**, 66–74.
15. Takashi, R., Muhlrad, A. & Botts, J. (1982) *Biochemistry* **21**, 5661–5668.
16. Marsh, D. J. & Lowey, S. (1980) *Biochemistry* **19**, 774–784.
17. Mendelson, R., Putnam, S. & Morales, M. (1975) *J. Supramol. Struct.* **3**, 162–168.
18. Ross, J. B. A., Schmidt, C. J. & Brand, L. (1981) *Biochemistry* **20**, 4369–4377.
19. Grinvald, A. & Steinberg, I. Z. (1974) *Anal. Biochem.* **59**, 583–598.
20. Badea, M. G. & Brand, L. (1979) *Methods Enzymol.* **61**, 378–425.
21. Paladini, A. A. & Weber, G. (1981) *Rev. Sci. Instrum.* **52**, 419–427.
22. Ikkai, T., Wahl, P. & Auchet, J.-C. (1979) *Eur. J. Biochem.* **93**, 397–408.